Electron differential cross section for H^--He stripping collisions

M. R. Franz, L. A. Wright,* and T. C. Genoni
Air Force Weapons Laboratory, Kirtland Air Force Base, New Mexico 87117
(Received 27 March 1981)

The Born approximation and a closure technique are employed to obtain the single and double differential cross sections for the ejected electron produced by electron detachment of H^- ions in collisions with He. Comparison is made to the recent measurements of Menendez and Duncan at 0.5 MeV. The theoretical results show that the experimentally observed structure in the double differential cross sections in the forward direction can be explained in terms of single-electron-loss processes alone.

Recently Menendez and Duncan[1] have measured the single and double (in energy and angle) differential cross sections (SDCS and DDCS, respectively) for the ejected electron in H^--He stripping collisions. Near 0°, the measured energy spectra exhibited a sharp cusplike peak with a second, broader peak on the low-energy side. The above authors tentatively interpreted the double-peak structure as resulting from two different processes, single- and double-electron loss (SEL and DEL, respectively). In the present work, we suggest an alternative explanation based on a calculation of only SEL processes.

Calculations of the SDCS and DDCS for the ejected electron have been performed for the collisional detachment process

$$H^-(1s^2) + He \rightarrow H(1s) + e^- + He^* . \tag{1}$$

The target atom He is initially in the ground state and He* indicates that the target-atom final state may be any bound state or a continuum state. Making use of the density of final states for a three-particle system, we obtain the following expression for the differential cross section:

$$\frac{d\sigma}{d\Omega_e dk_e} = \frac{4m_T\mu_{HT}}{v_i}\int \frac{|F^I(\vec{K})|^2 |F^T(\vec{K})|^2 k_e^2 k_H^3 d\Omega_H}{K^4[m_T k_H^2 + \mu_{HT}(\vec{k}_e\cdot\vec{k}_H - \vec{k}_i\cdot\vec{k}_H)]} . \tag{2}$$

In Eq. (2), v_i is the incoming velocity of the ion, m_T is the mass of the target atom, μ_{HT} the reduced mass of the resultant H atom and target, and $F^I(\vec{K})$ and $F^T(\vec{K})$ are the atomic form factors for the negative ion and target atom, respectively. $\vec{k}_i$ is the laboratory-frame momentum of the incoming ion, $\vec{k}_e$ and $\vec{k}_H$ are the final momenta of the ejected electron and H atom in the laboratory frame, respectively, and $\vec{K}$ is the momentum transfer

$$\vec{K} = \vec{k}_i - \vec{k}_H - \vec{k}_e . \tag{3}$$

The form factor for the negative ion is given in the Born approximation by

$$F^I(\vec{K}) = \langle \Psi_f | 1 - e^{-i\vec{K}\cdot\vec{r}_1} - e^{-i\vec{K}\cdot\vec{r}_2} | \Psi_i \rangle . \tag{4}$$

Ψ_i and Ψ_f are the initial and final eigenstates of the H^- ion and $\vec{r}_j$ is the coordinate of the jth electron relative to the center of mass of the H^- system. For the H^- ion, simple wave functions were used for both the bound and free states. The bound-state H^- wave function was taken to be the well-known two-parameter form[2]

$$\Psi_i(r_1, r_2) = N_i(e^{-\alpha r_1}e^{-\beta r_2} + e^{-\beta r_1}e^{-\alpha r_2}) \tag{5}$$

$$= \Psi_\alpha(r_1)\Psi_\beta(r_2) + \Psi_\beta(r_1)\Psi_\alpha(r_2) , \tag{6}$$

where N_i is the normalization constant, $\alpha = 1.04$, and $\beta = 0.24$. The final wave function for the H^- system was orthogonalized to the initial state by

$$\Psi_f = \tilde{\Psi}_f - \langle \tilde{\Psi}_f | \Psi_i \rangle \Psi_i . \tag{7}$$

In Eq. (8), $\tilde{\Psi}_f$ is the symmetrized product of a plane wave and the 1s hydrogenic orbital

$$\tilde{\Psi}_f(r_1, r_2) = 2^{-1/2}[\Psi_\kappa(r_1)\Psi_{1s}(r_2) + \Psi_{1s}(r_1)\Psi_\kappa(r_2)] , \tag{8}$$

where $\Psi_\kappa(\vec{r}) = (2\pi)^{-3/2}e^{i\vec{\kappa}\cdot\vec{r}}$ and $\vec{\kappa} = \mu_{eH}(\vec{v}_e - \vec{v}_H)$, the reduced mass of the electron times its final velocity relative to the resultant H atom.

The summation over final states of the target was accomplished using the closure approximation and an average momentum transfer in the manner described by Lee and Chan.[3] The form factor and incoherent scattering function for the target were obtained using a simple wave function for the He ground state and are given in Ref. 4. To check the accuracy of our computations and the validity of the closure approximation, previously reported H^--H scattering calculations[5] were repeated using the present formalism. (The results reported in Ref. 5 were obtained by explicitly summing over discrete and continuum final states of the target-H atom.) Results of the two calculations agreed to within 1%. This closure approximation will be discussed in more detail in a future publication.[6]

We now compare our present calculations to the experimental results of Menendez and Duncan

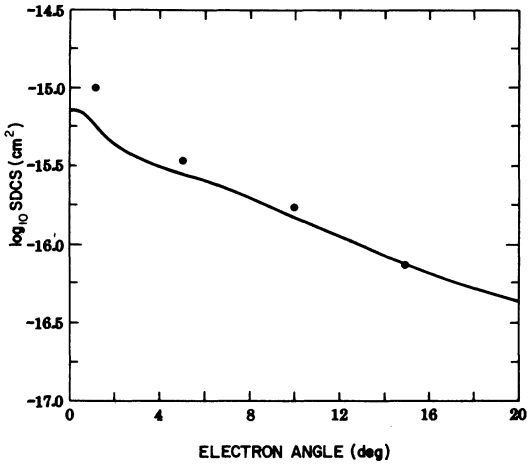

FIG. 1. Electron single differential cross section at 0.5 MeV for electron detachment of H^- on He. The full curve is the present result. The dots represent experimental data of Menendez and Duncan (Ref. 1).

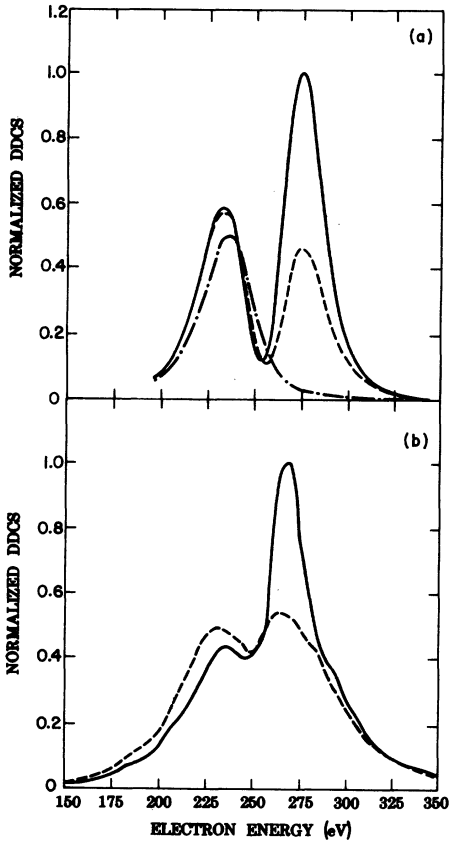

FIG. 2. (a) Theoretical electron double differential cross section at 0.5 MeV for electron detachment of H^- on He. The full curve represents an electron-scattering angle of 0.3°, the dashed curve, 1.5°, and the broken curve, 4.0°. (b) Experimental electron double differential cross section at 0.5 MeV for electron detachment of H^- on He (Ref. 1). The full curve represents an electron-scattering angle of 0.3°, the dashed curve, 1.5° (curves have been drawn through experimental data).

for an ion energy of 0.5 MeV and target-He atom. The SDCS is presented in Fig. 1. Even though the calculation does not include excited states of the resultant H atom or DEL processes, good qualitative agreement between theory and experiment is achieved for small scattering angles. As θ_e increases, the theoretical cross section becomes less reliable due to the breakdown of the Born and average momentum transfer approximations at large scattering angles. Figure 2(a) shows the theoretical DDCS for electron scattering angles of 0.3°, 1.5°, and 4.0°, and Fig. 2(b) the experimental DDCS for scattering angles 0.3° and 1.5°. The calculated DDCS in the forward direction reproduces all of the qualitative features of the DDCS observed in the experiments. The large peak, centered at $v_e \simeq v_i$, decreases with scattering angle and vanishes for $\theta_e \gtrsim 4.0°$. The theoretical DDCS also exhibits the broad peak at lower electron energy which, as was observed experimentally, moves to higher energies as the electron-scattering angle increases.

The behavior of the DDCS can be understood in terms of the H^- matrix elements involved. They are of the form

$$\langle \Psi_\alpha, \Psi_\beta | e^{-i\vec{K}\cdot\vec{r}_1} | \Psi_{ns}, \Psi_\kappa \rangle + \langle \Psi_\alpha, \Psi_\beta | e^{-i\vec{K}\cdot\vec{r}_1} | \Psi_\kappa, \Psi_{ns} \rangle + \langle \Psi_\beta, \Psi_\alpha | e^{-i\vec{K}\cdot\vec{r}_1} | \Psi_{ns}, \Psi_\kappa \rangle + \langle \Psi_\beta, \Psi_\alpha | e^{-i\vec{K}\cdot\vec{r}_1} | \Psi_\kappa, \Psi_{ns} \rangle . \quad (9)$$

The first and third terms are nondirectional and peak for $\kappa \simeq 0$ and K small. $\kappa \simeq 0$ necessarily implies small electron-scattering angles. These terms, therefore, account for the sharp cusplike peak in the DDCS near 0° which vanishes rapidly as the angle increases. They therefore contribute little to the total cross section. Physically, these terms describe collisions in which momentum is transferred to the resultant H atom and the electron proceeds undisturbed in the forward direction.

On the other hand, the second and fourth terms in Eq. (9) are directional and peak strongly for $\vec{K} \simeq \vec{\kappa}$. For small electron-scattering angles, $\vec{K}$ and $\vec{\kappa}$ are predominantly antiparallel to $\vec{k}_i$, so these terms give rise to a second peak at lower electron energy. For larger electron-scattering angles, $\vec{\kappa}$ is no longer antiparallel to $\vec{k}_i$ and the second peak is located at higher electron energies. These terms correspond to collisions in which momentum is transferred primarily to the ejected electron.

As was observed in Ref. 5, they dominate both the differential cross section for the resultant H atom and the total cross section.

In spite of the simple wave functions used and the approximations made, these calculations explain all the observed features of the double differential cross section in terms of single-electron loss. The existence and location of the two peaks and the disappearance of one peak at larger angles can all be explained without invoking double-electron-loss processes.

---

*Present address: Mission Research Corporation, 1400 San Mateo Blvd., SE, Suite A, Albuquerque, New Mexico 87109.

[1]M. G. Menendez and M. M. Duncan, Phys. Rev. A 20, 2327 (1979).
[2]S. Chandrasekhar, Astrophys. J. 100, 176 (1944).
[3]Y. T. Lee and J. C. Y. Chen, Phys. Rev. A 19, 526 (1979).
[4]J. H. Hubbell *et al.*, J. Phys. Chem. Ref. Data 4, 471 (1975).
[5]T. C. Genoni and L. A. Wright, J. Phys. B 13, 461 (1980).
[6]L. A. Wright, T. C. Genoni, and M. R. Franz (unpublished).